

Supporting Information

A High-Speed Multipass Coulter Counter with Ultra-High Resolution

Martin A Edwards[†], Sean R German^{†‡}, Jeffrey E Dick[§], Allen J Bard[§], Henry S White^{†*}

[†]Department of Chemistry, University of Utah, Salt Lake City, Utah 84112, United States

[‡]Revalesio Corporation, 1200 East D Street, Tacoma, Washington 98421, United States

[§]Center for Electrochemistry, Department of Chemistry, The University of Texas at Austin, Austin, Texas 78712, United States

*white@chem.utah.edu

Table of Contents

Current-Time Traces of 250 nm Radius Polystyrene Particles.....	S-2
Measuring of Blockages	S-3
Trapping for Extended Periods of Time	S-4
Electron Microscopy of Particles	S-6
Histograms of Percentage Current Blockage for Individual Particles	S-7
Current-Time Traces of a Mixture of 250 and 100 nm Polystyrene Particles.....	S-12
Termination of Trapping	S-14
Example of Trapping at High Frequency (200 Hz).....	S-18
Data Acquisition and Filtering.....	S-20
Diffusion Calculations and Probability of a Second Particle Entering the Nanopore	S-21

Current-Time Traces of 250 nm Radius Polystyrene Particles

The following plots show i - t traces for the particles from Figure 2a in the main text on an expanded current and time scale, such that individual particle translocations (spikes of \sim 5 nA amplitude) and switching events (current rapidly switching from \sim 240 nA to \sim -248 nA) are clearly resolvable. Translocations taken from the start, middle and end of the burst show the particle first entering the pipette, being successfully and stably trapped, before finally being pulled deep into the pipette after 101 measurements.

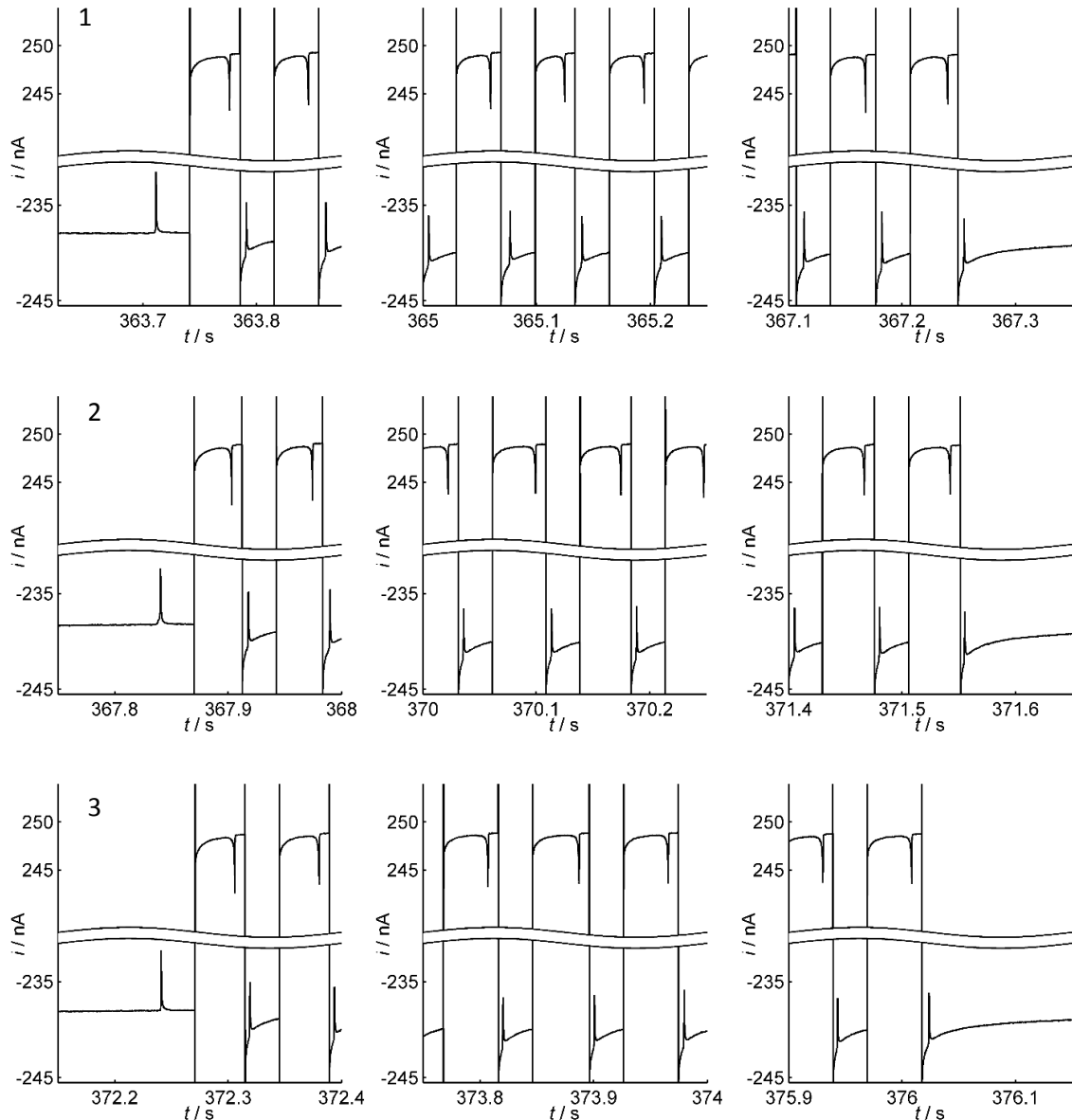


Figure S1. i - t traces on an expanded current and time scale of the 250 nm nominal radius polystyrene particles labelled 1, 2 and 3 in Figure 2a in the main text. Note the break in the i axis. Note: the top-left and top-right parts are reproductions from Figure 2b in the main text. 0.1 M NaCl with buffer, \sim 600 nm radius pipette

Measuring of Blockages

Current blockages were measured relative to the background current, which was determined by least-squares fitting a curve (dashed line) to the current as is shown in Figure S2. The region about the peak (black circles) and that including the charging current/switching region (blue circles) was ignored for the fitting. The red circle represents the deepest current blockage with the depth being indicated by the length of the red line (5.89 nA and 5.63 nA for the top and bottom plots respectively). The percentage blockage was calculated by dividing the blockage by the background value at the time of the blockage.

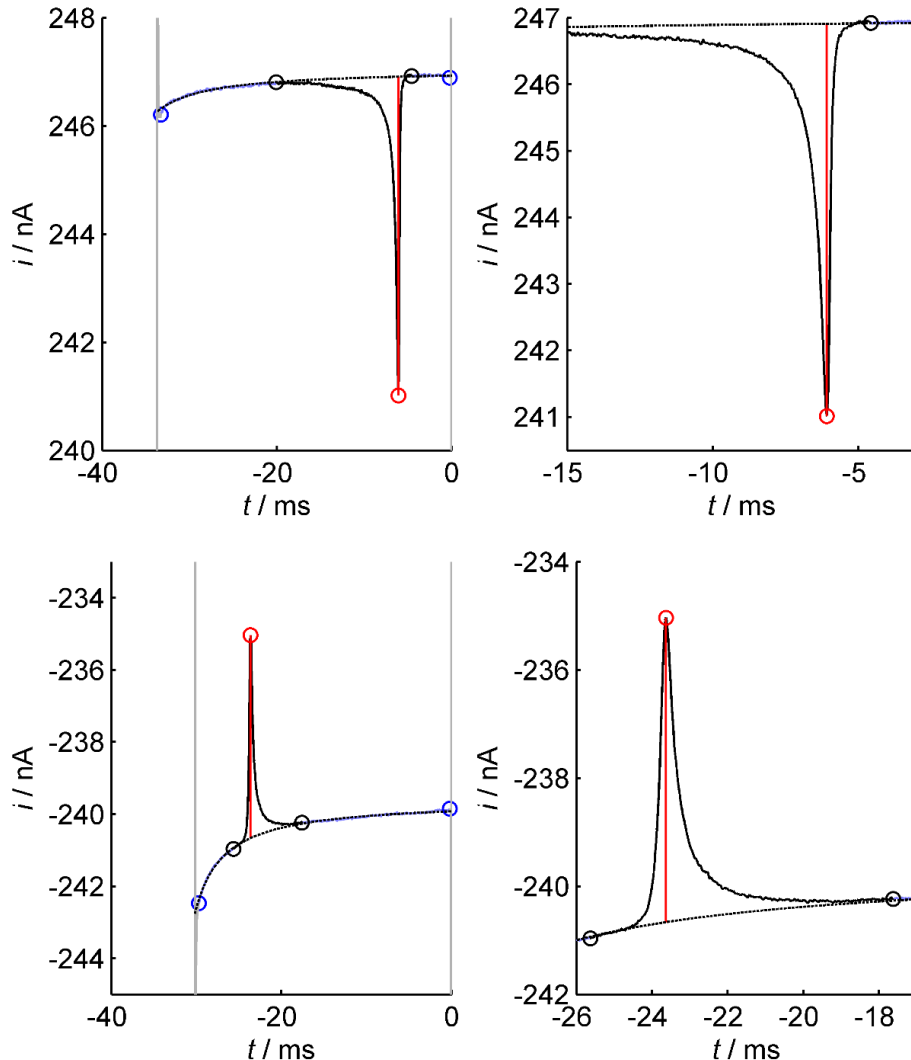


Figure S2. i - t traces showing background fitting and measuring of blockage percentages; right-hand side plots are an expanded plots of those on the left. Dashed line is the background fit. Blue circles denote the points from which the switching/charging currents were excluded from the background fit and the black circles where the resistive pulse was excluded. The red circle represents the point at which the blockage was measured, while its depth is indicated by the length of the red line. In each case $t=0$ is chosen as the switching time after the translocation. 0.1 M NaCl with buffer; ~600 nm radius pipette; 250 nm nominal radius particle.

Trapping for Extended Periods of Time

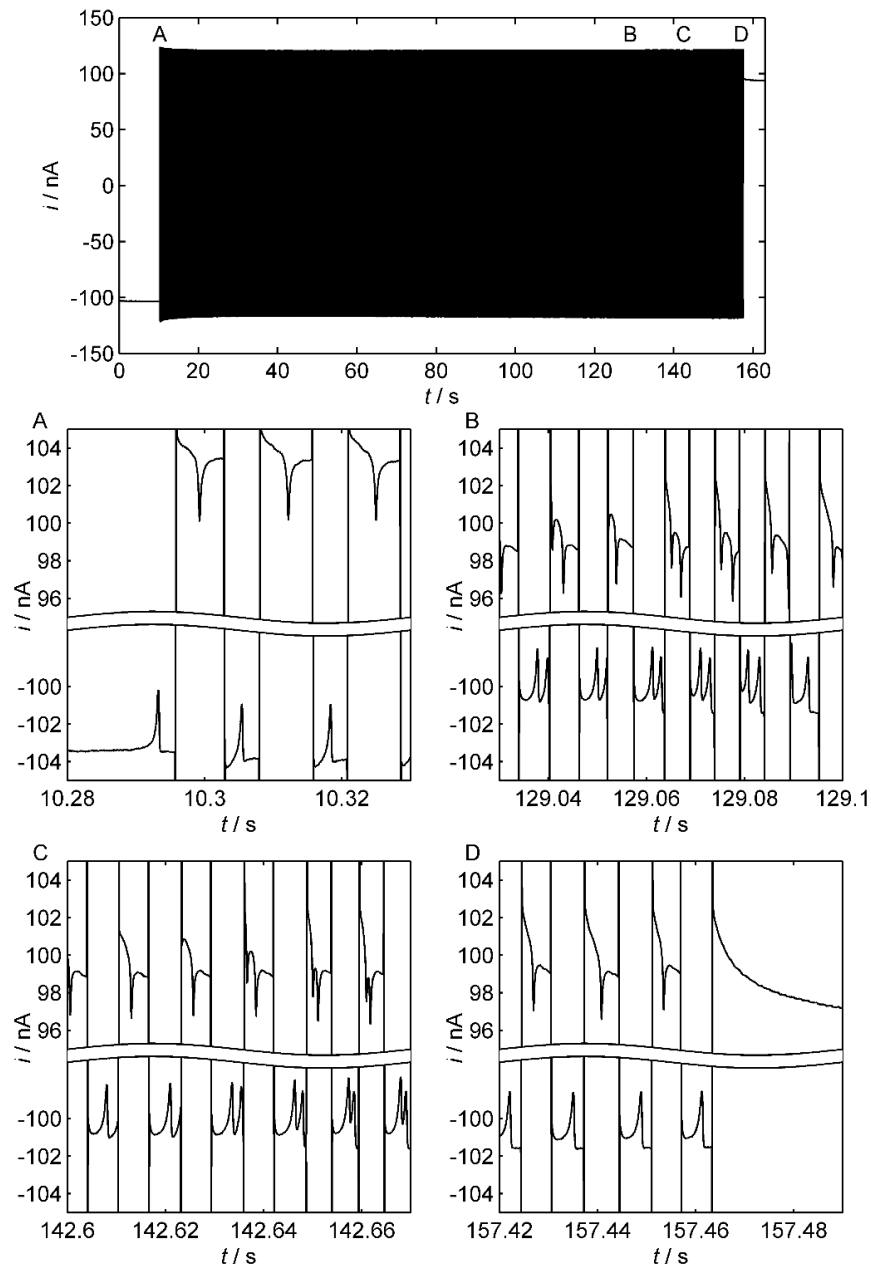


Figure S3. i - t trace for the voltage trapping/measuring of polystyrene particles (250 nm nominal radius) for ~ 145 s. Top plot shows the full time series. Lower plots are shorter traces coming from segments identified by letters in the initial plot. 50 mM NaCl with buffer, ~ 500 nm radius pipette.

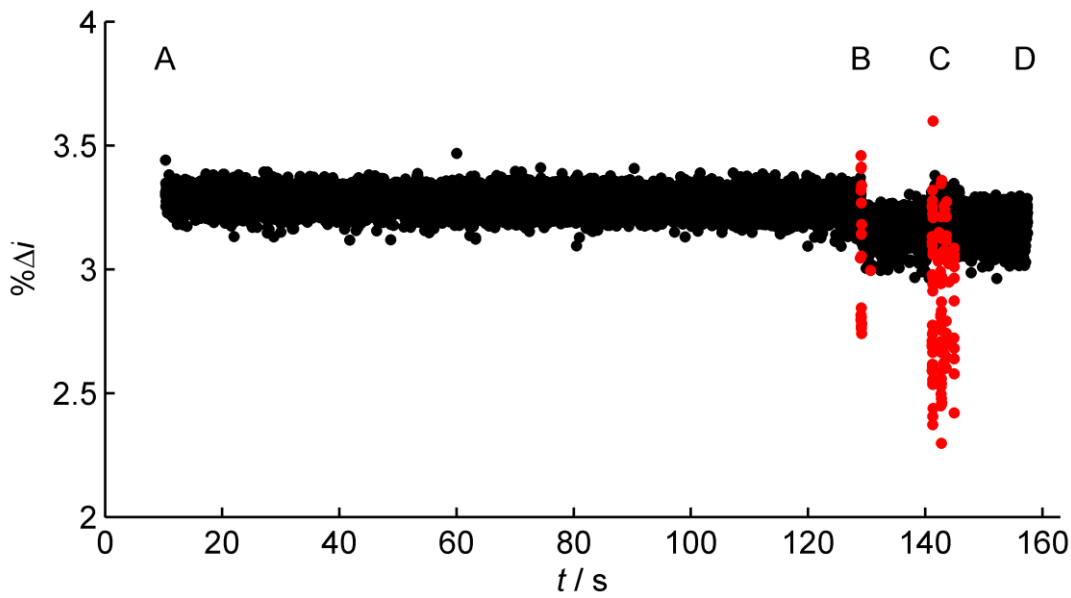


Figure S4. Plot of $\% \Delta i$ vs t for the inward translocations from the i - t trace shown in Figure S3. Points colored in red come from the periods when two particles were trapped (parts B and C in Figure S3) and are not included in subsequent analysis. 50 mM NaCl with buffer; \sim 500 nm radius pipette; 250 nm nominal radius.

Figure S3 and Figure S4 illustrate that we may trap a particle for an extended period of time taking many thousands of measurements and determining the mean current blockade to an exceptionally high resolution. In Figure S3 a particle first leaves the pipette at \sim 10 s (A), it translocates back-and-forth over 18,000 times before a second particle enters at around 129 s (B). This represents \sim 2 minutes that the particle was trapped and measured. The system returns to a single trapped particle after \sim 10 translocations. Figure S4, which shows $\% \Delta i$ for the trace in Figure S3, shows a clear change in the mean current level after the \sim 129 s, indicating that the particle in the trap changed. For the instance at \sim 143 s (C), where a second particle enters the trap for several 10s of translocations, no clear change in the mean current blockade is visible and we cannot be certain from this plot alone whether the particle in the trap has changed. However, the mean percentage current blockades of $3.275 \pm 0.001\%$, $3.169 \pm 0.005\%$, $3.182 \pm 0.006\%$ for these segments (10-129 s, 129-143 s and 143-157 s; error represents 3 S.E.M.) suggest that the particle in the trap may well have changed at \sim 143 s. The error of $\pm 0.001\%$ for the trap of 2 minutes is equivalent to a confidence interval of ± 31 pm on the radius (with the assumption that the particle is spherical); this is equivalent to considerably less than a monolayer over the entire particle.

Electron Microscopy of Particles

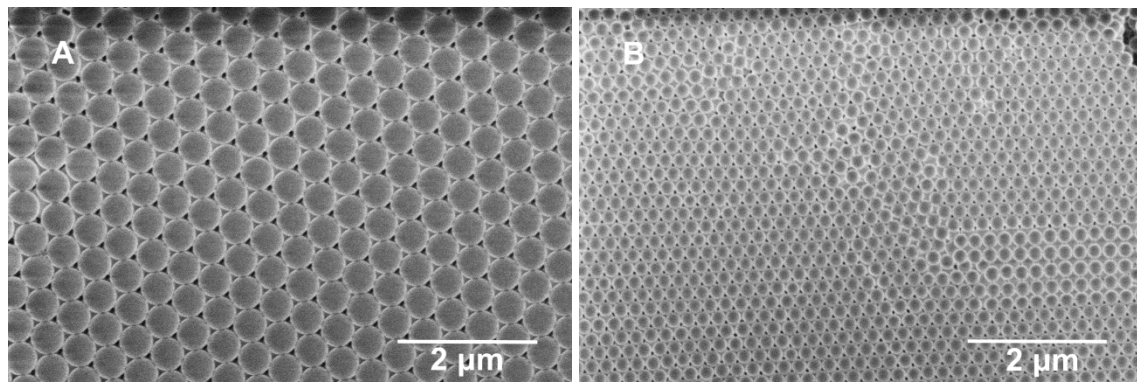
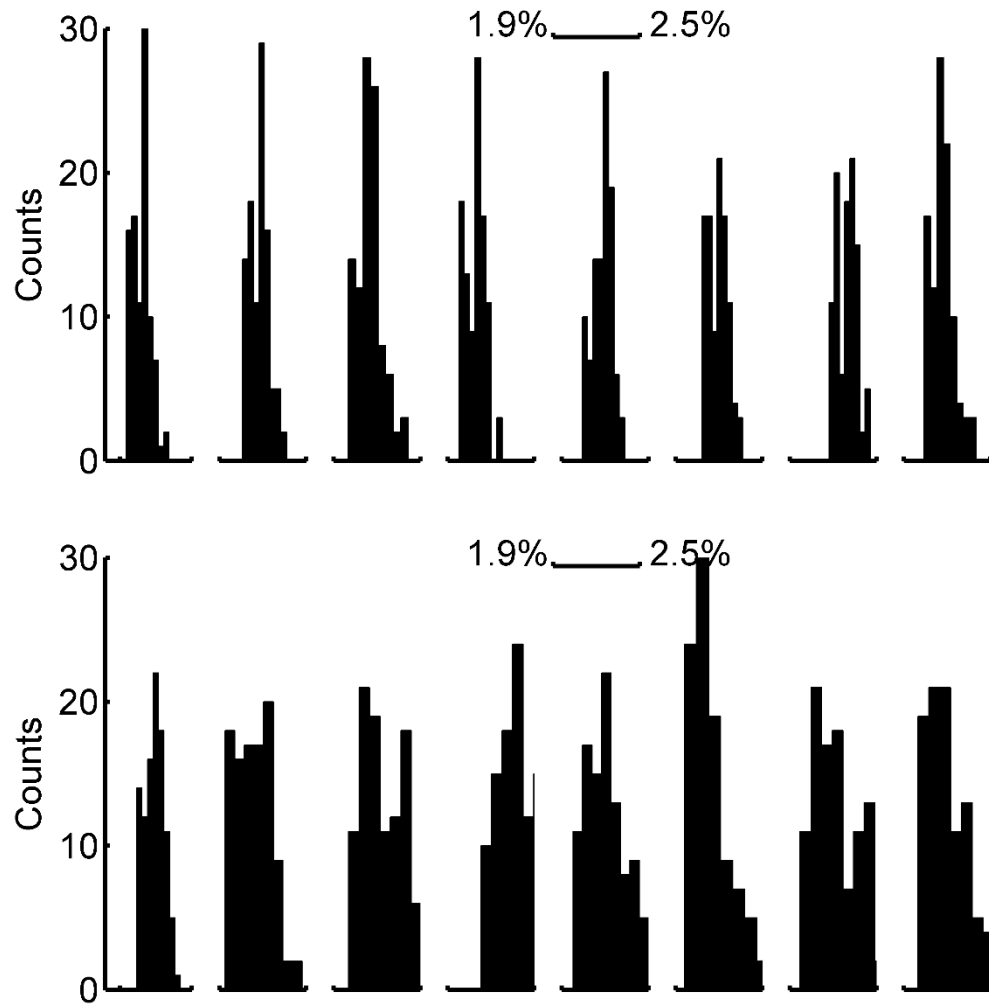


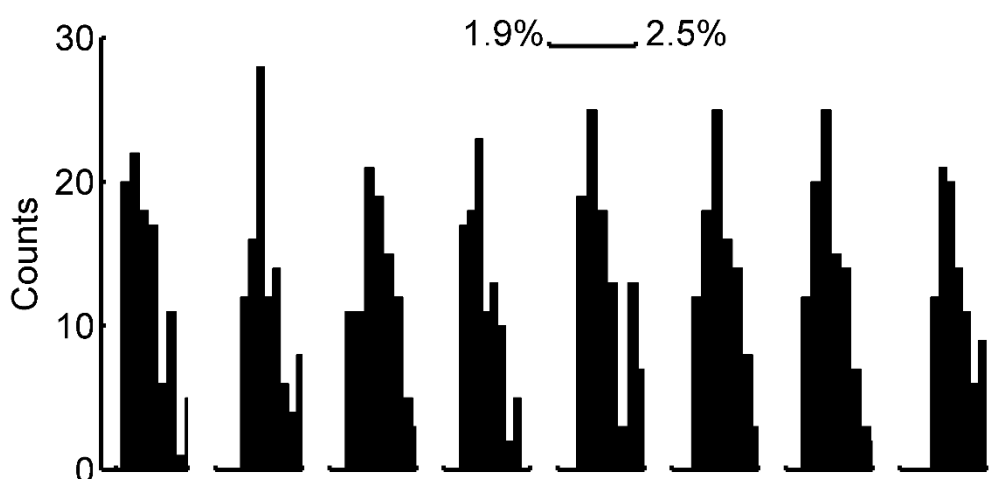
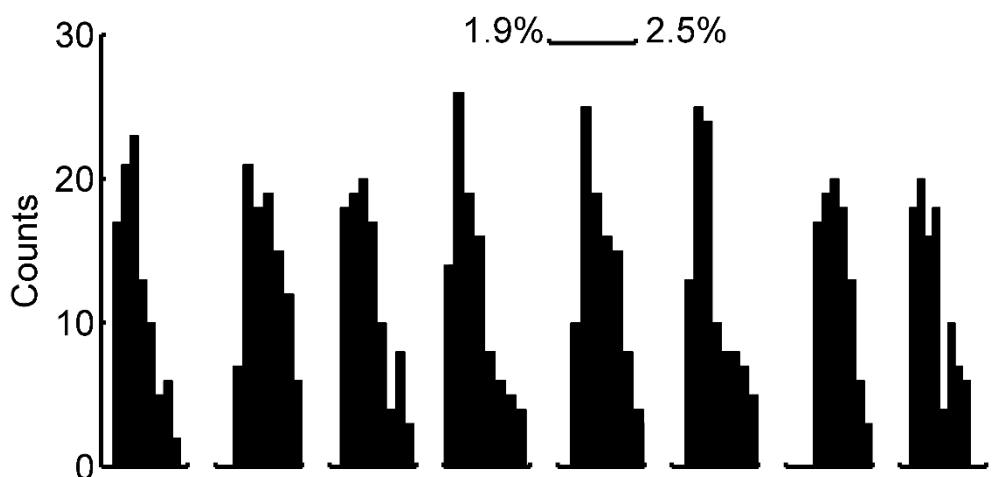
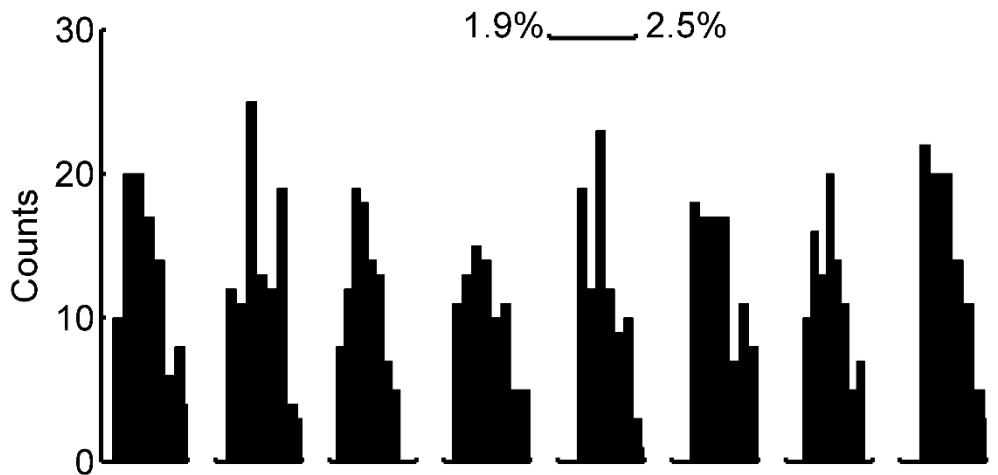
Figure S5. Scanning electron micrographs of (A) 250 nm and (B) 100 nm nominal radius polystyrene nanoparticles on silicon.

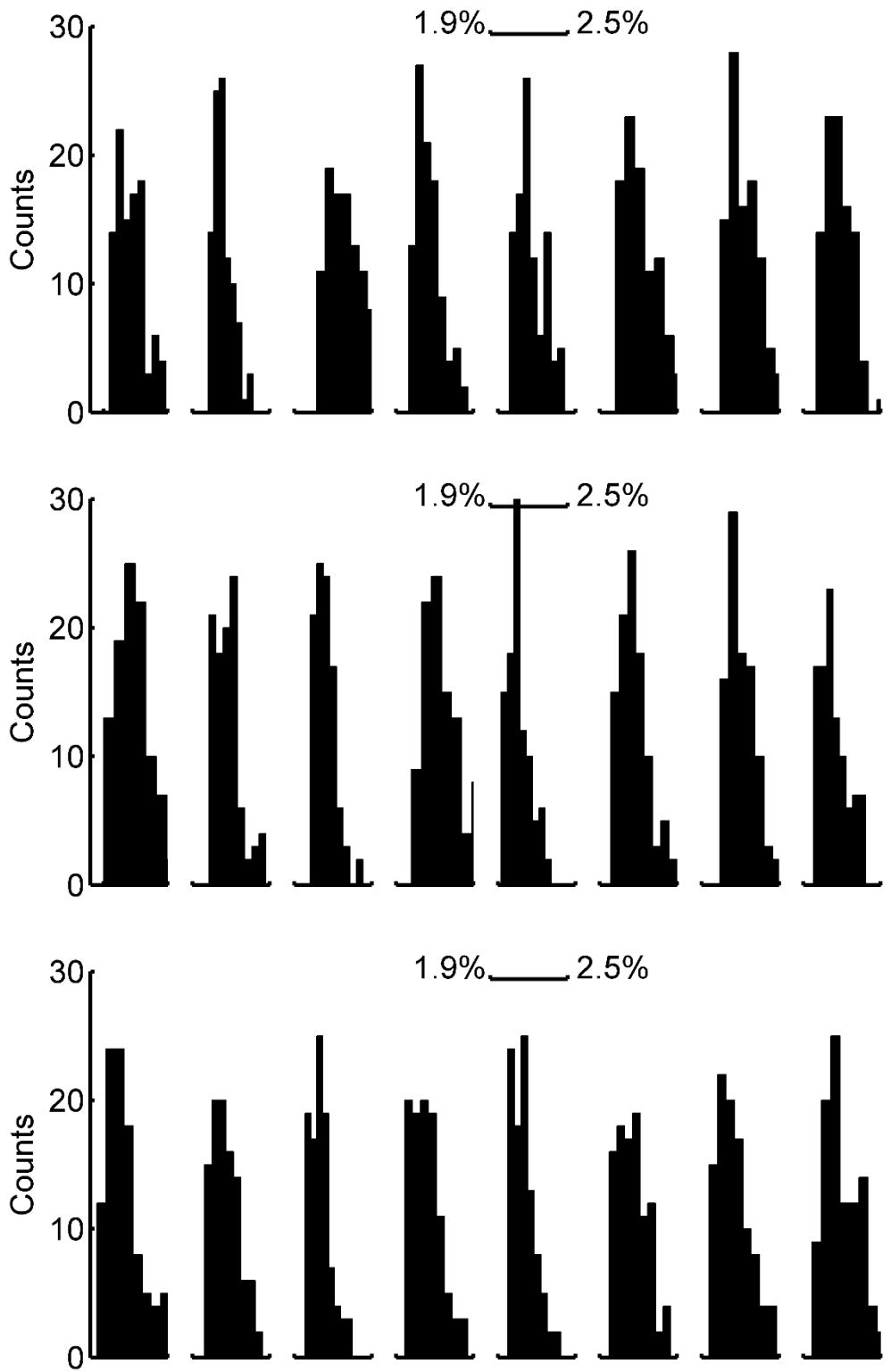
Scanning electron microscopy was used to determine the distribution of particle sizes. 10 μL of a 2.6% suspension of particles was placed onto silicon wafers and dried in an oven at 60 °C. Field Emission SEM images were captured with a FEI Helios Nanolab 650 (1 kV accelerating voltage) and are shown in Figure S5. Measurement of the radius of 50 particles each in (A) and (B) gave mean radii of 241 ± 3 and 108 ± 4 nm, respectively, corresponding to the 250 nm and 100 nm nominal radius particles.

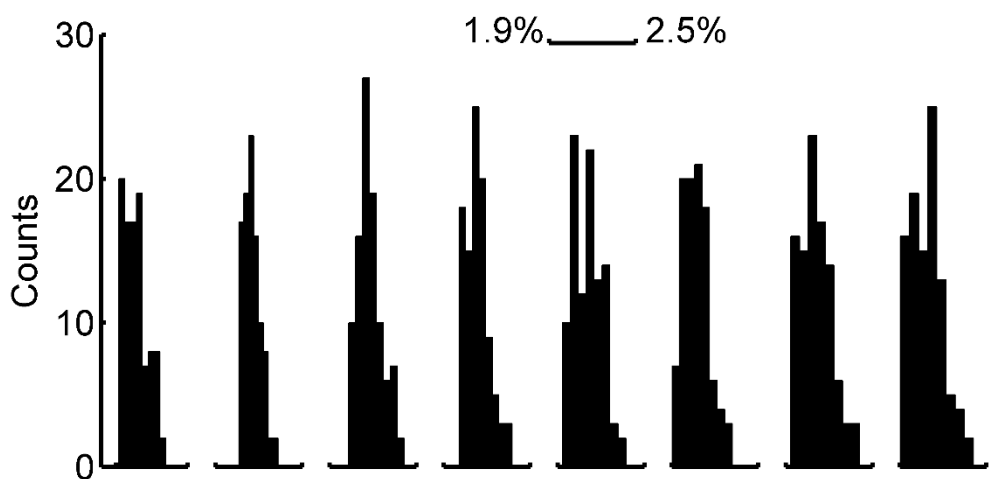
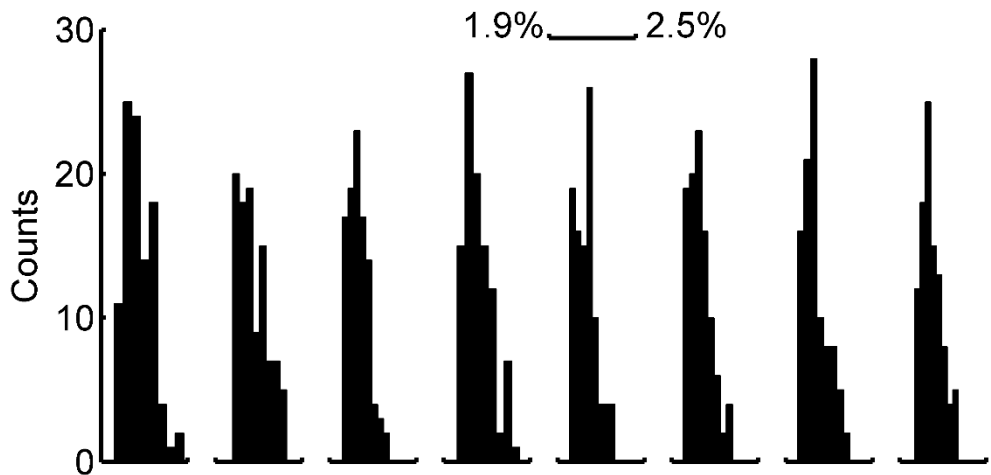
Histograms of Percentage Current Blockage for Individual Particles

Figure 4b in the main text presents a population histogram, that is, a histogram of the size of many particles, the size of each of which was *individually* characterized by 101 resistive pulse translocations. Each histogram below (Figure S6) corresponds to one of the polystyrene nanoparticles included in the Figure 4b histogram.









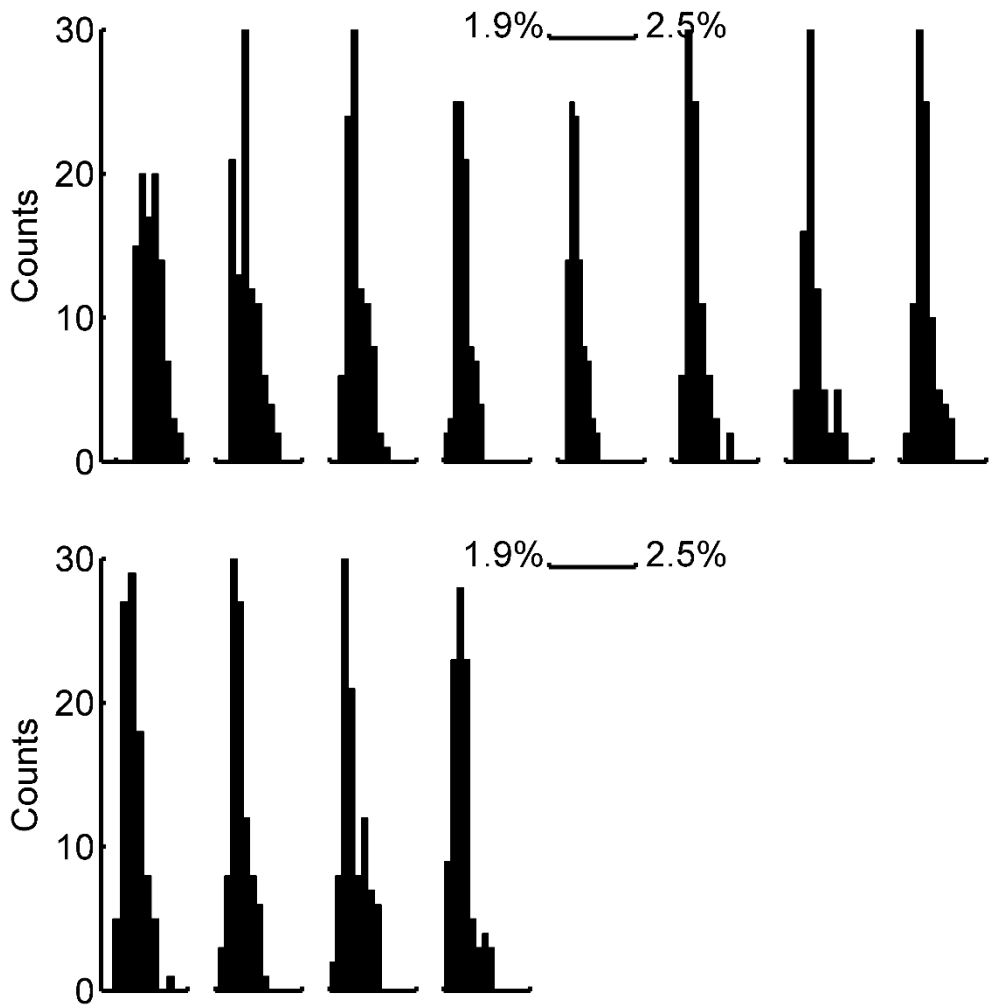
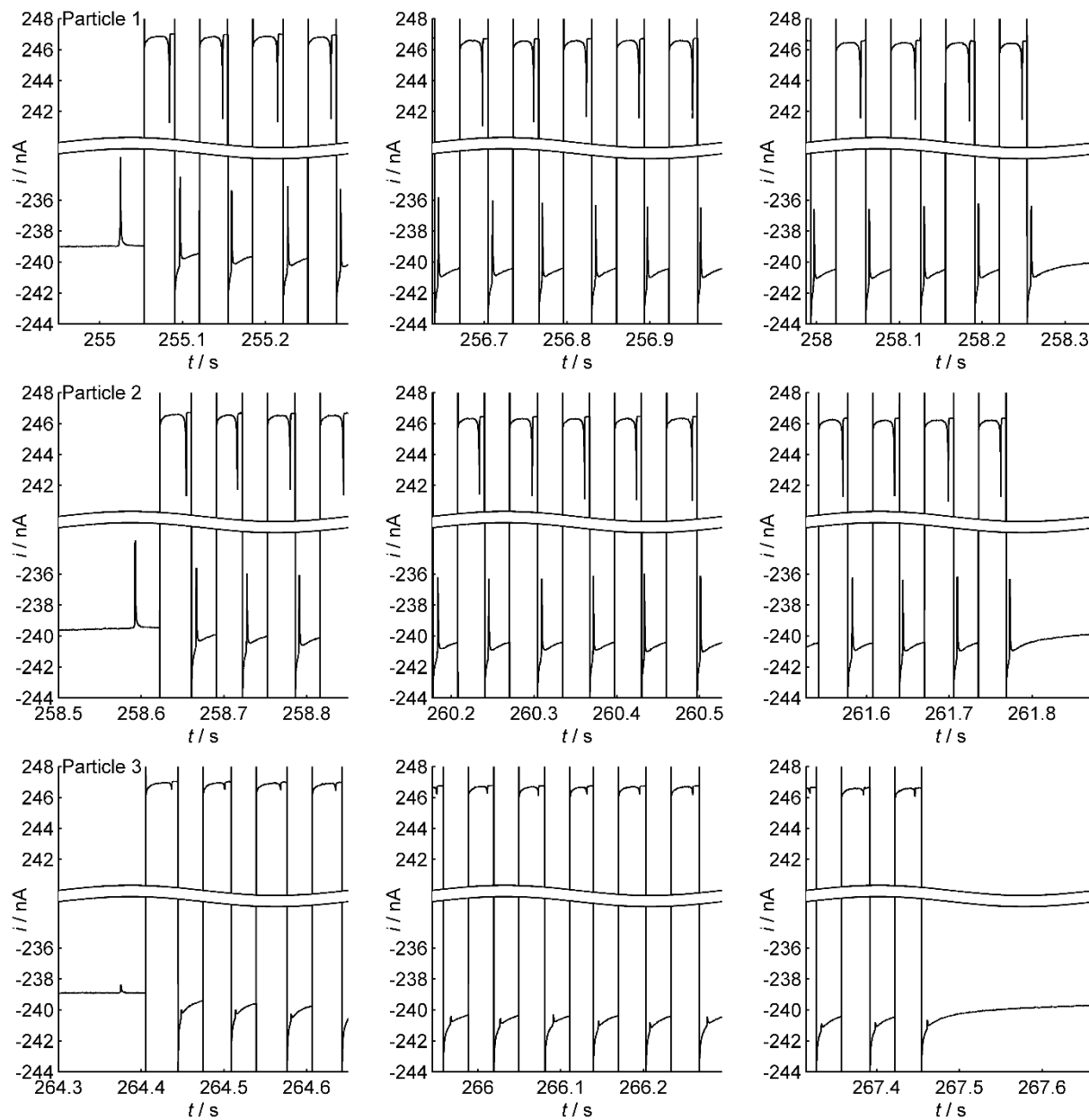


Figure S6. Histograms of the $\% \Delta i$ for the 92 of the 100 particles used to create the populations histogram shown in Figure 4b of the main manuscript (the other 8 particles are those shown in Figure 4a). As in Figure 4a, each histogram presents data corresponding to 101 translocations of the same 250 nm nominal radius polystyrene nanoparticle. 0.1 M NaCl with buffer, \sim 600 nm radius pipette.

Current-Time Traces of a Mixture of 250 and 100 nm Polystyrene Particles

It is possible to trap and measure particles of significantly different sizes using a voltage switching approach. Figure S7 shows data that were initially presented in Figure 5 of the main manuscript on expanded current and time axes. Each row shows the start, middle and end of the i - t traces for 6 different particles (3x100 nm nominal radius (particles 3, 4 & 6), 3x250 nm nominal radius (particles 1, 2 & 5)), each captured/measured for 101 translocations.



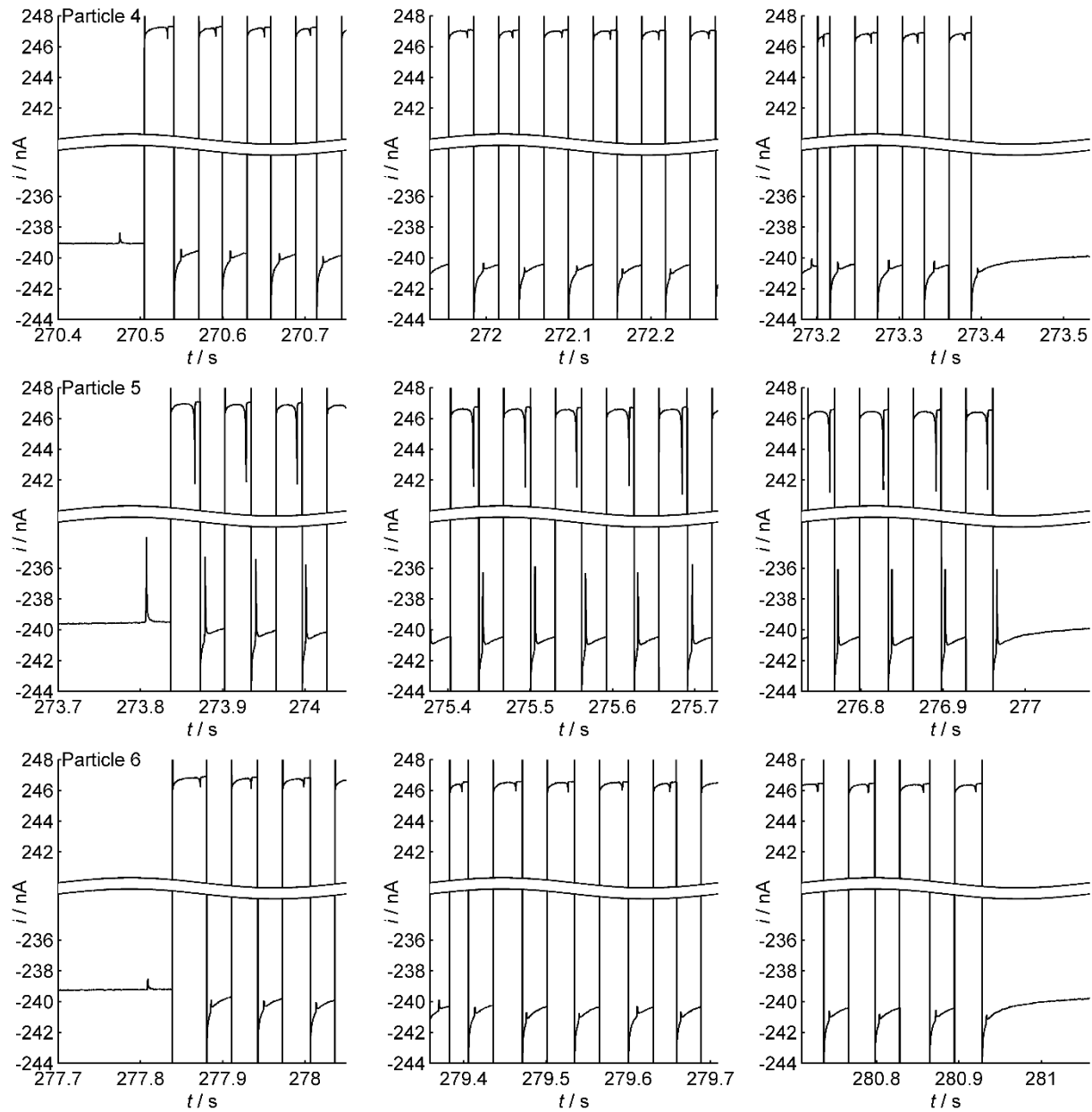


Figure S7. i - t traces from voltage trapping/measuring a mixture of 100 and 250 nm nominal radius polystyrene nanoparticles. Plots are of the data shown in Figure 5 of the main text, but on expanded current and time scales. 0.1 M NaCl with buffer, \sim 600 nm radius pipette.

Termination of Trapping

The trapping system has a number of user controlled parameters (trigger level, time to wait before switching the potential, time before rearming trigger, etc.) that should be adjusted for optimal performance. The following figures show examples of undesirable terminations of trapping, which are generally ameliorated by judicious choice of control parameters.

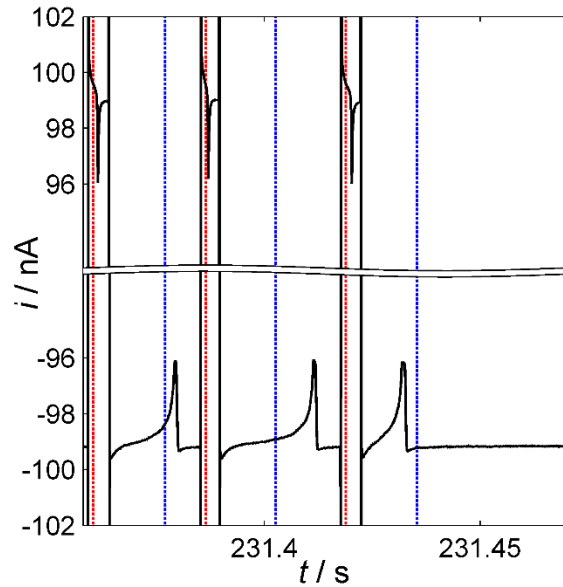


Figure S8. i - t trace showing the loss of a particle due to it exiting the pipette prior to rearming the trigger. Dashed vertical lines are the time at which the trigger was rearmed for positive (red) and negative (blue) polarities.

Figure S8 shows a i - t trace where a trapped particle is lost due to it exiting the pipette prior to the rearming of the trigger. There are three blockages shown at negative polarities, which from their asymmetry can be attributed to the particle leaving the pipette. The three blockages at positive polarities indicate particle entry into the pipette, although the asymmetry is difficult to assess on this scale. Despite switching the potential at a precise time after the particle is detected (2 ms after detection for positive polarity, 7 ms after detection negative polarity), each blockage occurs at a different time after the potential is changed due to Brownian motion. Vertical dashed lines indicate when the trigger was rearmed, blue for negative polarity (13 ms after switching) and red for positive polarity (1.3 ms after switching). The first two exits shown occur after the trigger is rearmed; they are detected and cause the potential to be switched. The third occasion where the particle is shown to exit at \sim 231.43 s occurs prior to the trigger being rearmed, the software continues to wait for the particle to exit the pipette and it is lost. Shortening the time to rearm the trigger, while avoiding and transient currents from switching, can overcome this problem. Alternatively, increasing the time taken before the particle exits, e.g., by changing the delay before switching, could reduce this problem. If too high a threshold is set for the triggering a particle may be lost in a similar manner; this can be resolved by lowering the threshold value.

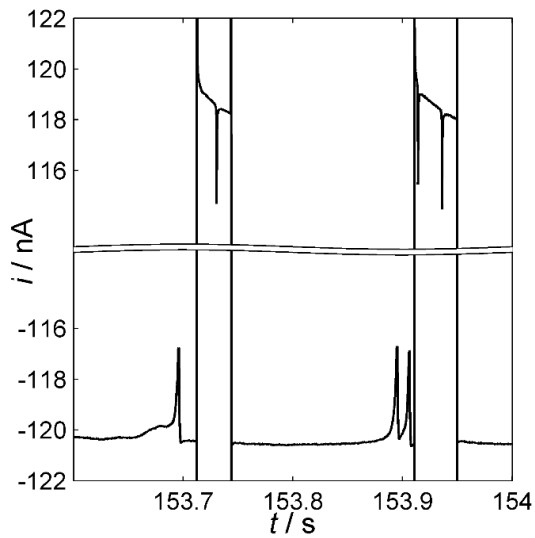


Figure S9. i - t trace showing a second particle passing through the pipette orifice prior to switching the potential.

Figure S9 shows a i - t trace where a trapped particle is joined by a second particle passing through the pipette orifice at ~ 153.9 s as can be seen by the two blockages in rapid succession. The two particles are visible as two separate blockages in the following segment at positive polarity. The entry of a second particle is a stochastic process occurring when a particle random walks close to the pipette. It is a function of the particle concentration, with more occurrences at higher concentrations. Working at moderately low particle concentrations, such as done in this work, reduces this problem. Practically, if we observe such an event with high frequency, we will dilute the solution using the buffer without particles. In this work, we reject all bursts that contain double events in our post analysis. A more detailed analysis of the likelihood of such events is presented in the section *Diffusion Calculations* in the Supporting Information

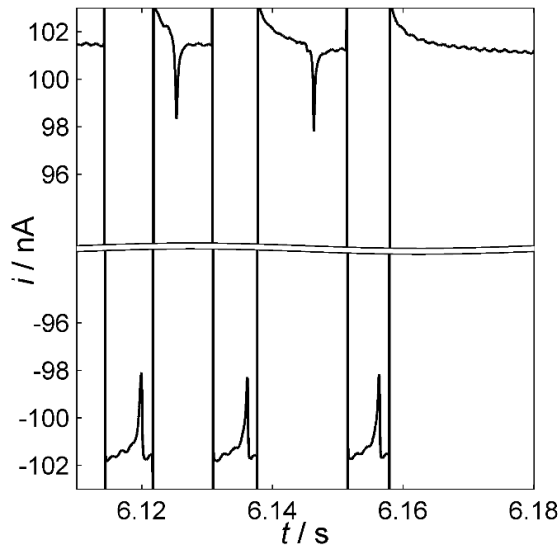


Figure S10. i - t trace showing a situation where a trapped particle exits a pipette, but is not recaptured.

Figure S10 shows a i - t trace showing a particle exiting the pipette at ~ 6.12 s, before performing two in-out cycles; however, at ~ 6.155 s, the particle exits the pipette and is not recaptured after reversing the potential. This may be explained by the particle undergoing a random walk beyond the sphere of influence of the applied voltage prior to the potential being switched. This is evidenced by an increasing probability of such a situation as the value t_{wait} for the particle outside the pipette is increased. Shortening this time reduces such a loss and appropriate choice of parameters can completely remove such phenomena as we see by trappings of multiple minutes ($>10,000$ trappings).

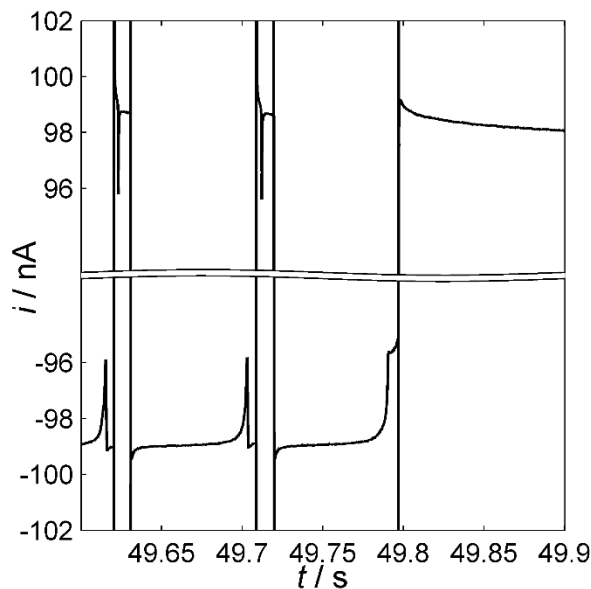


Figure S11. i - t trace showing a particle unable to translocate through the pipette prior to the potential switching.

Figure S11 shows a partial translocation just prior to 49.8 s. No particle is visible on the subsequent segment at a positive polarity as the particle was still at least partially inside the pipette when the potential was switched. While in some cases a partial translocation could be due to a very short time between detection and triggering (t_{wait}), which could easily be adjusted, in this case we see a plateau at the top of the resistive pulse suggesting that the particle stayed in approximately the same position. This event is typically very rare, unless the size of the pipette and particle are very closely matched and it is common to perform experiments for many hours without observing such a phenomenon.

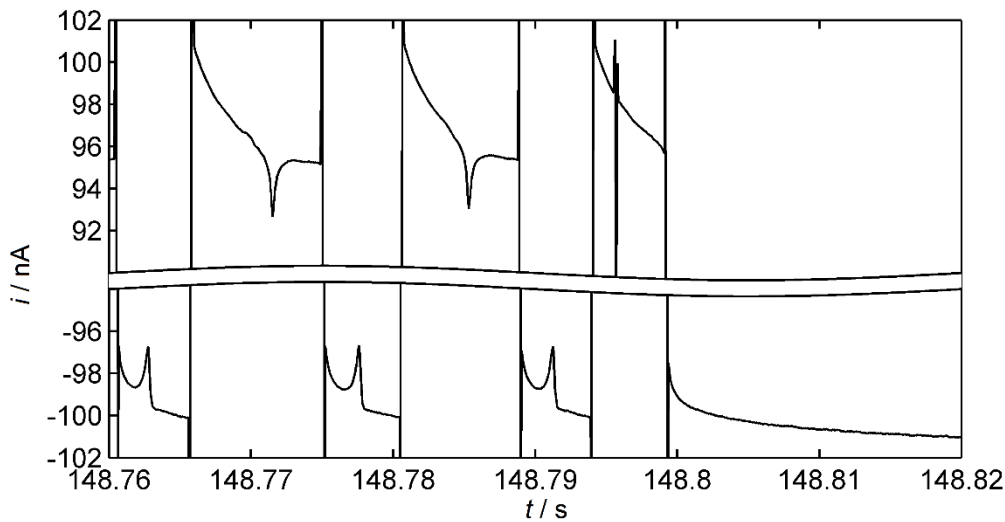


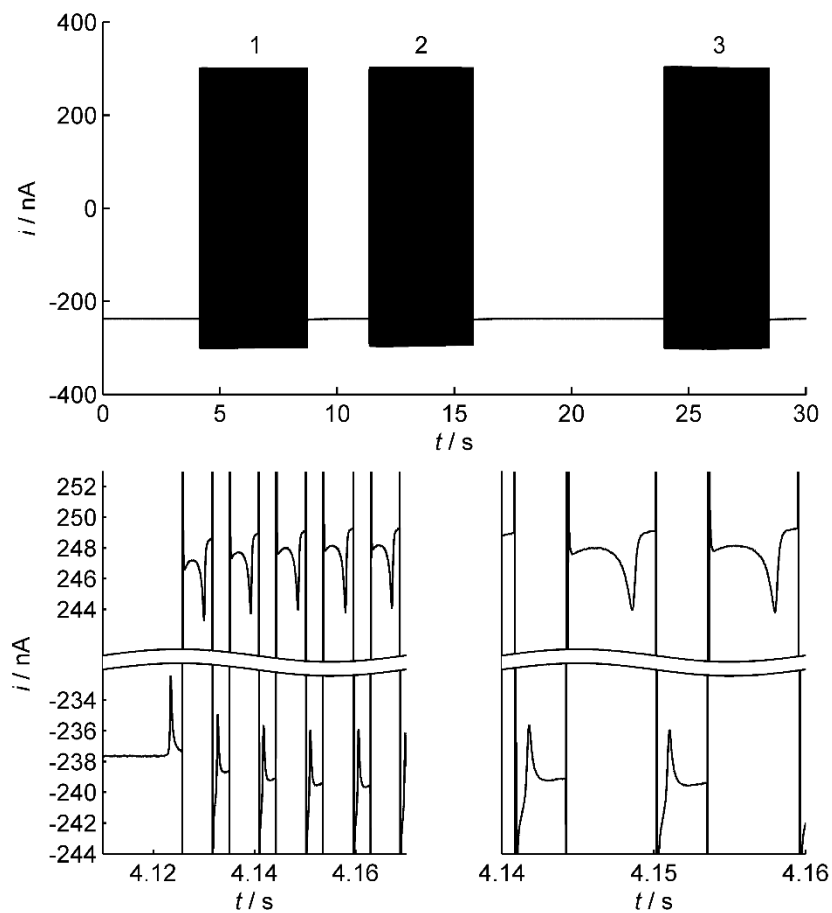
Figure S12. i - t trace showing a captured particle being lost due to premature triggering induced by extraneous noise.

Figure S12 shows an example of a trapped particle being lost due to premature triggering. In this case an external vibration caused a current spike which induced triggering and switching prior to the particle translocation. An appropriately isolated experimental system/environment can help avoid extraneous signals and hence, avoid this type of termination of a trapping. Setting a trigger threshold too low, such that it triggers off noise/background current changes, would also cause a similar termination to trapping.

Example of Trapping at High Frequency (200 Hz)

The use of high speed data acquisition and processing protocols allow rapid responses to particle translocations and precise switching. Figure S13 shows i - t traces of three particles being trapped/measured 1001 times by voltage switching at a frequency of \sim 200 translocation/s, a 20-fold increase over the pressure based trapping we previously presented. For this system we see that the particle translocation takes almost the entire period of the measurement and thus represents an upper limit for this particular measurement. However, increasing the forces through using a higher voltage should provide a means to overcome this and is currently being explored.

In practice, it becomes challenging to perform measurements where the translocations take almost the entire duration of a segment. In such situations the resistive pulse become convoluted by the background response, which is hard to determine; this is apparent in the translocations at a negative potential in Figure S13.



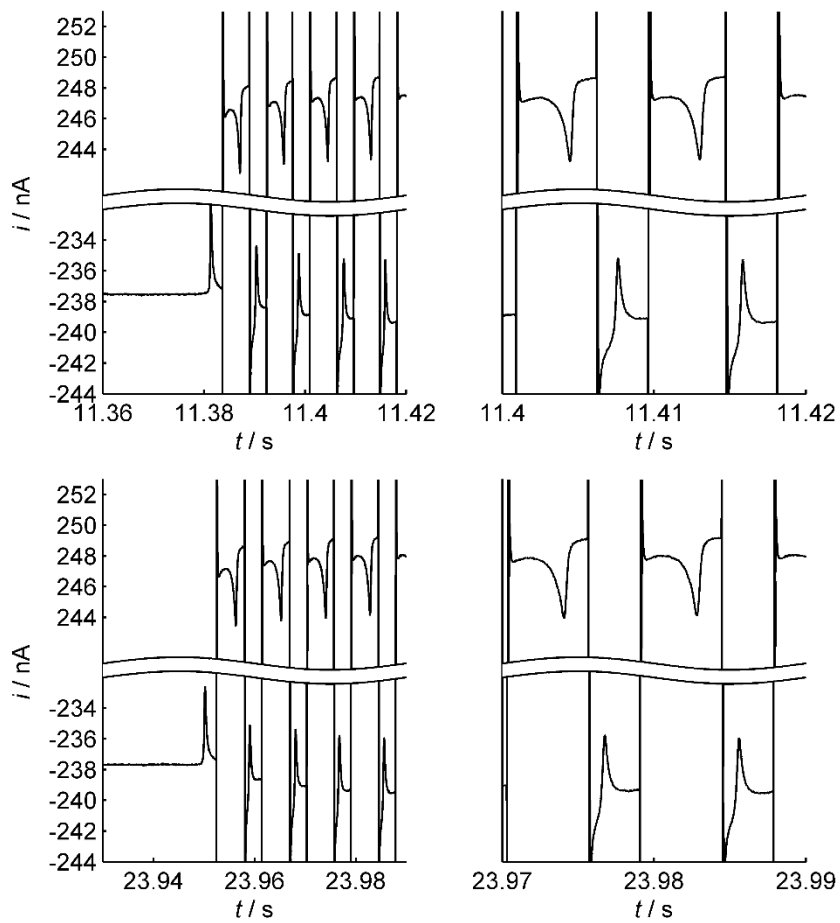


Figure S13. i - t traces of three 250 nm nominal radius polystyrene particles (500 nm nominal radius) undergoing voltage trapping/measuring 1001 times each at ~200 Hz. Data acquired at 30 kHz bandwidth; 0.1 M NaCl with buffer; ~600 nm radius pipette.

Data Acquisition and Filtering

All i - t in this paper were acquired with a Heka EPC10 USB patch-clamp amplifier at a frequency of 100 KHz and with either a 10 KHz or 30KHz Bessel filter applied. In each experiment the current range was chosen to minimize the impact of digitization.

Further post-filtering of i - t data was performed using a Savitzky-Golay finite impulse response (FIR) filter of polynomial order 3 and frame length 9. The filtering was implemented in Matlab using the command:

```
FilteredCurrent=sgolayfilt(RawCurrent, 3, 9)
```

where FilteredCurrent and RawCurrent are arrays containing the filtered and raw current data, respectively. Figure S14 shows that filtering reduced the noise drastically without distorting the peak shape. The unfiltered data shown in black show the same shape as the filtered data. The zoomed-in segments (RHS) show that even on this short time-scale distortion is practically absent.

With the exception of the black traces in Figure S14 all current-time data presented in this paper have been filtered as described above. Moreover, all statistical measurements (blockage percentages, etc.) were performed on the filtered data.

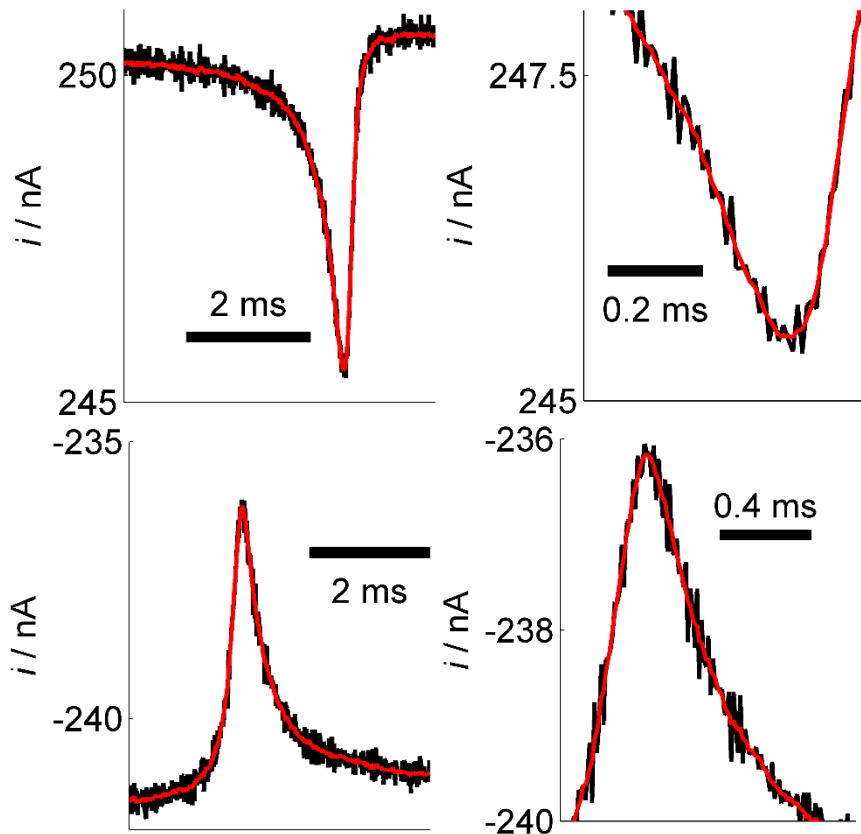


Figure S14. Raw (black) and filtered (red) i - t data for two representative translocations of a 250 nm nominal radius polystyrene particle. RHS plots are an expansion of those shown on the LHS.

Diffusion Calculations and Probability of a Second Particle Entering the Nanopore

The following calculations of diffusion coefficients and related quantities are provided to aid the reader. More precision may be gained with explicit simulation of random walks, but is beyond the scope of this work.

The diffusion coefficient, D , of a particles radius, r , can be calculated from the Stokes-Einstein relation (Equation S1)

$$D = \frac{k_B T}{6\pi\eta r} \quad (\text{S1})$$

where $k_B = 1.38 \times 10^{-23}$ J/K, $T = 293$ K, $\eta = 1e-3$ Pa s, and the radii for the 100 and 250 nm nominal radius particles as measured by SEM were $r = 108$ and $r = 241$ nm, respectively. This gives $D = 2.0 \times 10^{-12}$ m²/s and $D = 8.9 \times 10^{-13}$ m²/s for the 100 nm and 250 nm nominal radius particles, respectively.

Using these calculated diffusion coefficients we can calculate a characteristic diffusion length, d , using

$$d = \sqrt{6Dt} \quad (\text{S2})$$

where the factor of 6 implies we are considering 3-dimesional diffusion. For a typical time 10 ms, equating to 100 Hz trapping we get $d = 345$ or 231 nm for the 100 nm and 250 nm nominal radius particles, respectively.

The concentrations of 5×10^7 - 2×10^9 particles/ml equate to $1/5 \times 10^7 = 2 \times 10^{-8}$ to $1/2 \times 10^9 = 5 \times 10^{-10}$ ml/particle

These volumes are equivalent to a box of $\sqrt[3]{10^{-6} \times 2 \times 10^{-8}} \approx 2.7 \times 10^{-5}$ m to $\sqrt[3]{10^{-6} \times 5 \times 10^{-10}} \approx 7.9 \times 10^{-6}$ m length side (10^{-6} prefactor necessary for unit conversion).

Next we calculate the likelihood of a second particle becoming trapped while we are making a measurement. We first make the observation that while the forces due to the electric fields/fluid flow are varying with time, as the trapped particle is maintaining its average position, at the orifice, the time averaged force is approximately zero. Next, as the particles are initially only in the external solution, we recognize that this problem is no different than addressed by Kwon *et al.*¹ They address the collision frequency of nanoparticles with a disk in a plane where particles either adhere or ‘bounce’ off the electrode. The collision frequency in the latter case is comparable to our situation as we only load particles in the external solution.

Kwon *et al.* present the following relations where M is the particle mass, A the electrode (or in our case pipette orifice) area, c the particle concentration and f_{coll} the collision frequency.

$$V_{RMS} = \sqrt{\frac{3k_B T}{M}} \quad (\text{S3})$$

$$V_{RMS} = \frac{\delta}{t} \quad (\text{S4})$$

$$f_{coll} = \frac{\delta A c}{4\tau} \quad (\text{S5})$$

δ and t are step length and period, respectively. Using the density of polystyrene ($\sim 1.05 \text{ cm}^3/\text{g}$) and the formula for a volume of a sphere we get the mass of the 250 nm nominal radius particle as $M = 6.2 \times 10^{-17} \text{ kg}$. For a typical 400 nm radius pipette and a particle concentration of $8 \times 10^7 \text{ particles/ml}$ that would give $f_{coll} = 0.15 \text{ particles/s}$. For these conditions $\sim 1/7$ of the $\sim 1\text{s}$ duration 100-traps would be expected to be interrupted by a second particle entering the pore. As we observed such events less frequently ($\sim 1/20$ for these conditions) it suggests some of our numerical approximations are slightly inaccurate.

¹ Kwon, S. J.; Zhou, H.; Fan, F.-R. F.; Vorobyev, V.; Zhang, B.; Bard, A. J. Stochastic Electrochemistry with Electrocatalytic Nanoparticles at Inert Ultramicroelectrodes-Theory and Experiments. *Phys. Chem. Chem. Phys.* **2011**, *13*, 5394–5402.